Recovery of rare earth elements from electronic waste by diffusion dialysis

Zineellabidine Hammache, Sofiane Bensaadi, Yassine Berbar, Nathalie Audebrand, Anthony Szymczyk, Mourad Amara

Recovery of rare earth elements from electronic waste by diffusion dialysis

Z. Hammache[1,2], S. Bensaadi[1], Y. Berbar[1], N. Audebrand[2], A. Szymczyk[2 *], M. Amara[1]

[1] *Laboratory of Hydrometallurgy and Molecular Inorganic Chemistry, Faculty of Chemistry, USTHB, BP 32, 16111 Algiers, Algeria.*

[2] *Univ Rennes, CNRS, ISCR, Institut des Sciences Chimiques de Rennes, UMR6226, 35000 Rennes, France.*

*Corresponding author: anthony.szymczyk@univ-rennes1.fr

Abstract

Recycling rare earth elements (REEs) contained in electronic waste is of utmost importance due to their ever-increasing use in the high-tech sector. In this context, the use of non-polluting techniques represents a real challenge for scientists. In this work, we demonstrated that a clean and energy-efficient process, diffusion dialysis, has great potential for the recovery of neodymium (Nd) and praseodymium (Pr), contained in the Nd-Fe-B magnets of end-of-life computer hard disk drives (HDDs). Four kinds of polymer membranes were prepared by blending cellulose triacetate (CTA) and polyethylenimine (PEI) with the addition of di-(2-ethylhexyl) phosphoric acid (D2EHPA), tridodecylamine (TDDA), trioctylamine (TOA) or trioctylphosphine oxide (TOPO). The membranes were first characterized by several techniques such as water uptake, contact angle, ATR-FTIR, SEM, XRD and zeta potential. They were further implemented in diffusion dialysis experiments in which diluted HDDs leachates were used as feed solutions. The relevance of the diffusion dialysis process for the recovery of REEs was demonstrated as it was possible to extract up to 15% of the boron by spontaneous diffusion through the CTA / PEI / TOA membrane in 6 hours with a lab-scale cell operating in batch mode. All membranes were positively charged under the operating conditions and then, REEs (present mainly in the form of trivalent cations Nd^{3+} and Pr^{3+}) were strongly rejected. A fairly good correlation was found between the membrane water uptake and boron transfer, with boric acid molecules passing more easily through the more hydrated membranes. The selectivity factor between boron and REEs resulted from the interplay between the membrane structure, its water uptake ability and surface charge. It was also found to be dependent on the leachate

composition. The CTA / PEI / TDDA membrane was found to exhibit the greatest B / REE selectivity factors, with values reaching up to 3706 and 140 for Nd and Pr, respectively. The lower selectivity towards Pr was explained by the weaker Gibbs energy of hydration of Pr^{3+} cations compared with Nd^{3+}.

Keywords: Rare earths; polymer membranes; dialysis; Nd-Fe-B magnet; recovery.

1. Introduction

Global demand for rare earth elements (REEs) continues to increase due to their numerous applications in the high-tech sector [1]. Conventional ores cannot satisfy the staggering demand for these strategic elements. REEs are found in computers hard-disk drives (HDDs) [2], wind turbines, Ni – metal hydride batteries, luminophores, acoustic transducers, magnetic separators, hybrid cars, etc [3,4]. Recycling of neodymium (Nd) from end-of-life consumer products has attracted growing interest [5]. In this regard, several studies focused on the recovery of neodymium and praseodymium (Pr) from Nd-Fe-B permanent magnets contained in HDDs [6,7]. Nd-Fe-B magnets typically contain ~30 wt. % REEs. Besides Nd, several other REEs, such as Pr, Dy, Tb, Gd and Ho, may be found in Nd-Fe-B magnets [8,9].

Several REEs recovery techniques have been used, such as flotation [10], magnetic separation [11], complexation [12] or solvent extraction [13–15]. In this context, membrane processes have also been considered in recent years. Some studies dealing with the extraction and separation of REEs used liquid membranes [16]. A bubbling organic liquid membrane extraction using primary amine N1923 was used to extract and enrich low concentration REEs from leaching solutions of rare-earth ores [17]. Low-concentration REEs were also extracted using a bubbling organic liquid membrane with un-saponified P507 [18]. Nanofiltration membranes [19,20], dispersion micro-extractor membranes [21,22] or hollow-fiber membrane extractor [23] were also considered in recovery options of REEs.

Diffusion dialysis is a well-established process for the separation of chemical species in solution [24]. It is based on the application of a concentration difference between two compartments separated by a membrane. It is a clean technique that does not require the addition of chemicals and it is energy-efficient as no hydraulic-pressure difference is applied through the membrane. Both the membrane features (e.g. pore size, surface charge density, nature of surface functional groups, etc.) and the feed solution composition impact the separation efficiency [25,26]. Dialysis polymer membranes synthesized from mixtures of cellulose triacetate (CTA) and polyethyleneimine (PEI) were shown to be low-cost materials with good separation performance [27,28]. The addition of PEI has been widely used as it allows to form a charged layer on the membrane surface [29]. Furthermore, PEI can form complexes with heavy metals [30]. The addition of carriers, such as di-(2-ethylhexyl) phosphoric acid (D2EHPA), tridodecylamine (TDDA), trioctylamine (TOA) and trioctylphosphine oxide (TOPO), in liquid membranes and polymer inclusion membranes has been successfully applied to selective extraction of metal ions [31,32]. It is worth mentioning that D2EHPA and TOPO have also

been found efficient to extract REEs by liquid / liquid extraction [33-35]. Although D2EHPA, TDDA, TOA and TOPO have been used as carriers in liquid membranes and polymer inclusion membranes, their chemical structure with a hydrophobic alkyl backbone and one or several polar groups give them also plasticizing properties [36,37], which allows improving the membrane mechanical properties.

In this study, we investigated the possibility of recovering REEs (Nd and Pr) from electronic waste (Nd-Fe-B permanent magnets) using diffusion dialysis as a clean alternative process to liquid / liquid extraction [38]. Four dialysis CTA / PEI membranes containing D2EHPA, TDDA, TOA or TOPO were first synthesized. The membranes were further characterized by water uptake, water contact angle, Fourier-transform infrared spectroscopy in attenuated total reflectance mode (ATR-FTIR), X-ray diffraction analysis (XRD), scanning electronic microscopy (SEM) and zeta potential. Eventually, the four membranes were implemented in dialysis experiments and their ability to separate boron from REEs was evaluated.

2. Materials and methods

2.1. Chemicals

Cellulose triacetate (CTA), polyethyleneimine (PEI) (50%), di-(2-ethylhexyl) phosphoric acid (D2EHPA) (97%), tridodecylamine (TDDA) (97%), trioctylamine (TOA) (98%), trioctylphosphine oxide (TOPO) (98.5%), nitric acid (HNO_3) (65%), hydrochloric acid (HCl) (37%), potassium hydroxide and chloroform (99.8%) were purchased from Sigma Aldrich.

2.2. HDD magnet leaching

Magnets contained in the HDD of end-of-life desktop and laptop computers (Table 1) were first collected and demagnetized in a muffle furnace at 250 °C [39]. After crushing and fine grinding, the powder obtained from each magnet was weighed with an analytical balance before leaching in 3N HCl and HNO_3 solutions.

Table 1. HDDs features.

HDDs	Company	Model	Reference S/N	Country
Desktop	Western Digital	WD200 20gb	WD200EB-00BHF0	Malaysia
Laptop	Seagate	Momentus 5400,6 160 GB	5VC5SKY3	China

The leachates composition was determined by inductively coupled plasma mass spectrometry (ICP-MS; Thermo Fisher, model ICAP RQ). Ten replicas were performed.

2.3. Membrane preparation

The membranes were synthesized by the solvent-evaporation method [40-43]. CTA and PEI were dissolved separately in $CHCl_3$ with vigorous stirring for 2 h at room temperature. The two polymer solutions were then mixed and left under stirring for 3 h before adding D2EHPA, TDDA, TOA or TOPO. Stirring was pursued for another 2 h until a homogeneous solution was obtained. The latter was poured into a glass Petri dish (130 mm diameter) and left to evaporate the solvent for 24 h. Membranes in the form of homogeneous films were obtained and detached from the bottom of the Petri dish by gently adding a little water. It was observed that the addition of D2EHPA, TDDA, TOA or TOPO to the CTA / PEI led to much less brittle membranes, which confirmed that these compounds can act as plasticizers [36, 37]. Details of the amount of solvent as well as polymer and additive concentrations used for each membrane (labelled M1, M2, M3 and M4) are presented in Table 2.

Table 2. Amount of solvent, polymers and additives used in membrane preparation.

Membrane ID	$CHCl_3$ (mL)	CTA (wt. %)	PEI (wt. %)	D2EHPA (wt. %)	TDDA (wt. %)	TOA (wt. %)	TOPO (wt. %)
M1	20	33.34	22.22	44.44	/	/	/
M2	20	33.34	22.22	/	44.44	/	/
M3	20	33.34	22.22	/	/	44.44	/
M4	20	33.34	22.22	/	/	/	44.44

The chemical structures of CTA, PEI and additives used for membrane preparation are shown in Figure 1.

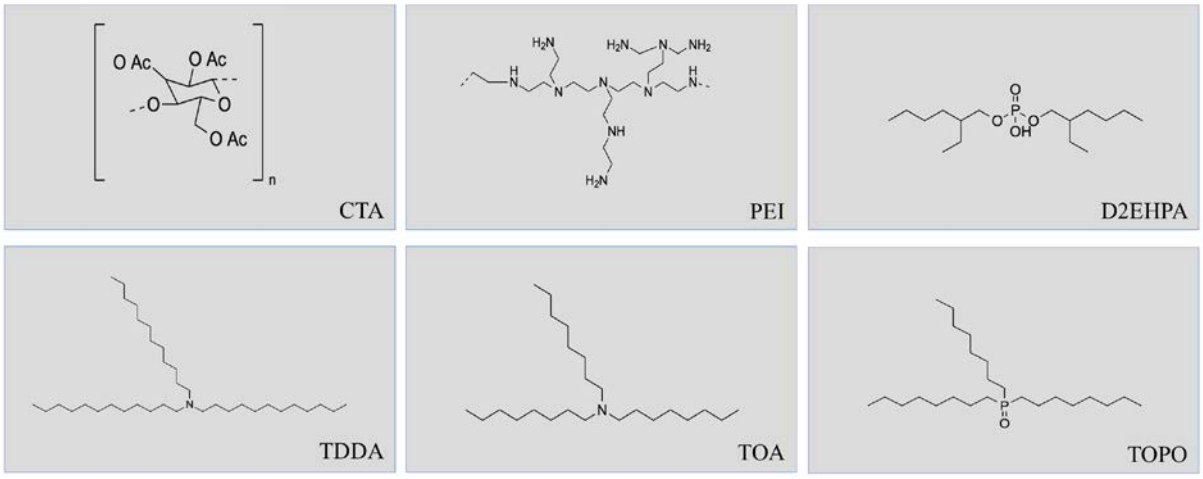

Figure 1. Chemical structures of CTA, PEI, D2EHPA, TDDA, TOA and TOPO.

2.4. Membrane characterization

2.4.1. Water uptake

A dry membrane sample (surface area: 4 cm^2) of known mass was soaked in deionized (DI) water for 24 h under gentle stirring. The membrane sample was then removed, wiped with absorbent paper and weighed [28]. The water content T (%) was determined by the following equation:

$$T = \frac{(m_w - m_d)}{m_d} \times 100 \quad (1)$$

where m_w and m_d are the mass of the wet and dry membrane sample, respectively.

2.4.2. Water contact angle

Contact angles were determined by the sessile-drop method using a DIGIDROP GBX-DS apparatus. A syringe was used to deposit DI water droplets with controlled size. Contact angles were determined by means of a video capture system and the Windrop++ software. The reported contact angles are the average of 10 measurements performed at different locations on the membrane surface. Measurements were performed at room temperature. Membrane samples were vacuum-dried for 48 h prior to measurements.

2.4.3. Attenuated Total Reflectance- Fourier Transform Infrared spectroscopy (ATR-FTIR)

The ATR-FTIR spectra of membranes were recorded using a PerkinElmer Spectrum™ 100 FTIR spectrometer equipped with a single-reflection diamond crystal (incidence angle: 45°). Each spectrum was averaged from 20 scans in the range 600−3700 cm^{-1} at a resolution of 2 cm^{-1}. Membrane samples were vacuum-dried for 48 h prior to analysis.

2.4.4. Scanning electronic microscopy (SEM)

Membrane surface morphology and membrane cross-section were characterized by SEM using a JEOL (JSM-7100 FEG EDS EBSD Oxford) microscope. For cross-section imaging, membrane samples were fractured after soaking in liquid nitrogen. Membrane samples were coated with an Au/Pd alloy prior to analysis.

2.4.5. *X-ray diffraction analysis (XRD)*

XRD analysis was performed with a Bruker D8 Advance diffractometer with Cu $K\alpha_1$ radiation (λ= 1.5406 Å) selected with an incident beam Ge (111) monochromator and equipped with a LynxEye detector in the 2θ range 10–80°. An adhesive tape was used to properly fix the

membranes on the sample holder. An additional in-depth structural analysis was carried out in the 2θ range 3–45° with both the M4 membrane and TOPO powder.

2.4.6. *Zeta potential*

A SurPASS electrokinetic analyzer (Anton Paar GmbH) was used to determine the surface zeta potential of the various membranes from tangential streaming current measurements [44]. The streaming current technique was preferred over the streaming potential to avoid any potential contribution of the electrical conduction through the membrane thickness [45]. Measurements were carried out at room temperature with a 1 mM KCl background solution in the pH range 3-9 (the pH was set by addition of 0.05M HCl and KOH solutions). Data were analyzed with the Visiolab software.

2.5. Diffusion dialysis

A lab-made diffusion-dialysis cell was used. The membrane (effective surface area: 15 cm^2) was sandwiched between two compartments of 85 mL each. The stripping and feed compartments were filled with DI water and diluted leachate, respectively. The leachates were diluted until a pH of ∼4 was reached so as to limit the hydrolysis of the acetyl groups of CTA (the hydrolysis rate is at a minimum in the pH range of 4–6) [46, 47] while keeping the membrane surface positively charged (see below). The increase in pH resulting from leachate dilution led to the precipitation of iron(III), which was further removed by filtration.
Dialysis experiments were performed in a batch-configuration for 6 h at room temperature. The feed and stripping solutions were stirred at 400 rpm to limit establishment of boundary layers. The solution composition was determined by ICP-MS by regularly withdrawing 0.2 mL volumes from both compartments. The transport yield of species *i* (η_i) was calculated by the following equation:

$$\eta_i = \frac{(C_{i,F}(0) - C_{i,S})}{C_{i,F}(0)} \times 100 \qquad (2)$$

where $C_{i,F}(0)$ is the initial concentration of species *i* in the feed compartment and $C_{i,S}$ is the concentration of *i* transferred to the stripping compartment. The volume change is the cell

compartments did not exceed 0.2 mL and was then neglected in the calculation of the transport yield.

The selectivity factor ($SF_{B/REE}$) [48], calculated by equations (3), was used to quantify the membrane efficiency for the selective separation of boron (B) and REEs (Nd and Pr):

$$SF_{B/REE} = \frac{C_{B,S}/C_{B,F}}{C_{REE,S}/C_{REE,F}} \quad (3)$$

where $SF_{B/REE}$ is the selectivity factor between boron and an REE (Nd or Pr), $C_{B,S}$ and $C_{B,F}$ are the concentration of boron in the stripping and feed compartments, respectively, $C_{REE,S}$ and $C_{REE,F}$ are the concentration of REE (Nd or Pr) in the stripping and feed compartments, respectively.

3. Results and discussion

3.1. Composition of Nd-Fe-B permanent magnets

The mass of the Nd-Fe-B magnet was 17.66 g and 2.88 g for the desktop-computer and laptop-computer HDDs, respectively. The composition of leachates obtained after leaching of Nd-Fe-B magnets is given in Table 3. The main component found in HDDs leachates was iron (~60-65 wt. %), followed by Nd (~20-28 wt. %). A significant difference in Pr (this element is always found with Nd) was detected in the two types of HDDs, with a much larger amount found in the laptop HDD (16.06 wt. % vs. 5.31 wt. %). The amount of boron (the third essential component in Nd-Fe-B magnets) was found between ~1 and 4 wt. %. Only a few traces of the light REEs, La, Ce, Sm and Eu, have been quantified in HDDs leachates. Results collected in Table 3 are in line with data reported in the literature [8,49].

Table 3. Composition of leachates (wt. %) obtained after leaching of Nd-Fe-B magnets. Confidence level: 95 %.

	B	Fe	La	Ce	Pr	Nd	Sm	Eu
Desktop	1.30	65.39	0.01	0.01	5.31	27.97	0.01	n.d.
Laptop	3.95	59.63	0.14	0.01	16.06	20.19	0.01	0.01

n.d.: not detected.

3.2. Membrane characterization

The water uptake and contact angle of the various membranes are reported in Table 4.

Table 4. Water uptake and contact angle of the various membranes.

Membrane ID	Water uptake (wt. %)	Contact angle (°)
M1	9.1	67.8 ± 1.5
M2	20.3	67.6 ± 1.3
M3	23.1	59.7 ± 3.8
M4	6.4	75.5 ± 0.8

The membranes incorporating phosphorus-based additives (M1 and M4) exhibited much less water uptake than their counterparts with amino additives (M2 and M3). M3 and M4 membranes exhibited the greatest and lowest water uptake, respectively. These results were correlated with water contact angles as M3 and M4 were found to be the most and least hydrophilic membranes, respectively. However, no such correlation was observed with M1 and M2 membranes, for which quite different water uptakes but similar contact angles were obtained.

Figure 2 shows the ATR-FTIR spectra of the various membranes. M1, M2 and M3 membranes exhibit the characteristic bands of CTA / PEI blend membranes. The band at 1747 cm^{-1} is associated with stretching of the C=O bond of CTA ester groups [50]. The characteristic bands of PEI are located around 1635 cm^{-1} (NH_2 bending from primary amines) and 1035 cm^{-1}

(stretching of the C-N band) [51,52]. The band around 1240 cm^{-1} results from stretching contributions of both C-O single bonds (CTA) and C-N from tertiary amines (PEI) [50,53].

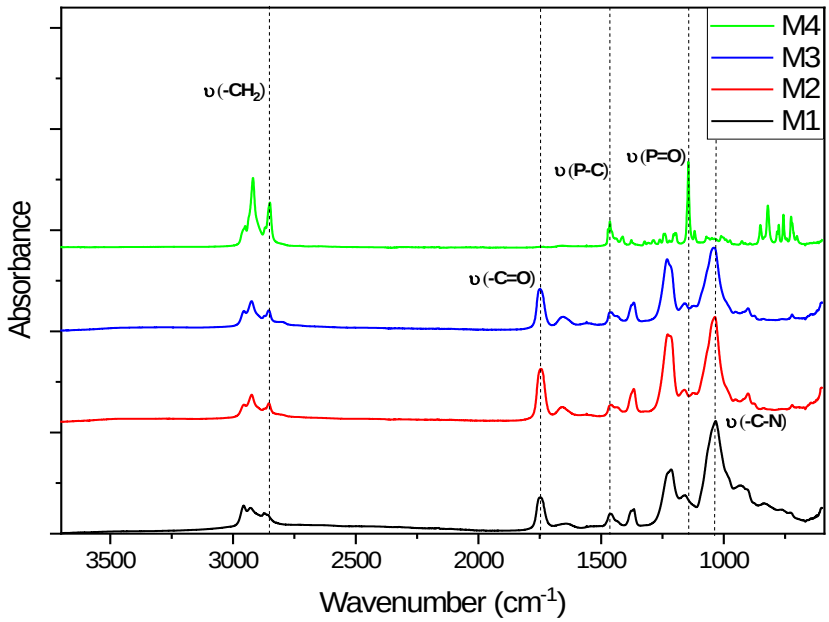

Figure 2. ATR-FTIR spectra of the various membranes (M1-M4) in the range 600-3700 cm^{-1}.

Strikingly, the ATR-FTIR spectrum of the M4 membrane did not show any of the above-mentioned characteristic bands of CTA and PEI. On the other hand, the spectrum showed the characteristic bands of TOPO. Indeed, the bands at 1154 and 1476 cm^{-1} correspond to the stretching vibrations of the P=O and P-C bonds of TOPO, respectively [53]. It is also worth noting the greater intensity of the bands associated with stretching of $C(sp^3)$-H (~2850-3000 cm^{-1}) compared with the other membranes. These results indicate that TOPO was not homogeneously distributed in the bulk of the membrane and that it was preferentially located on the membrane surface, forming a layer thicker than the penetration depth of the IR beam, which is in the µm range. It was most likely the result of the bad affinity between TOPO and $CHCl_3$, which led to migration of TOPO towards the membrane surface during the slow solvent evaporation process.

Conclusions drawn from ATR-FTIR were confirmed by SEM. Figure 3 shows the cross section of the M1 and M4 membranes. Unlike the M1 membrane, which showed a relatively homogeneous (sponge-like) structure, a several micrometer-thick layer can be seen on the M4 membrane surface. The TOPO layer formed on the surface may also explain why the M4 membrane had the highest water contact angle of the four membranes (Table 4).

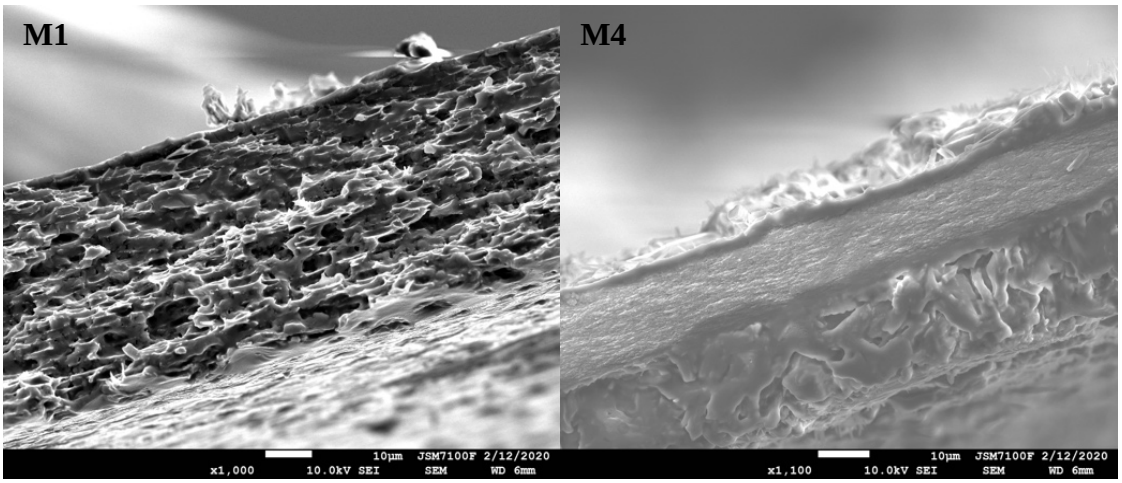

Figure. 3. SEM images of the M1 (left) and M4 (right) membranes cross-sections (scale bar: 10 μm).

The surface of all membranes was found to be dense without pores (see for instance the SEM images of the surface of M2 and M3 membranes in Figure 4).

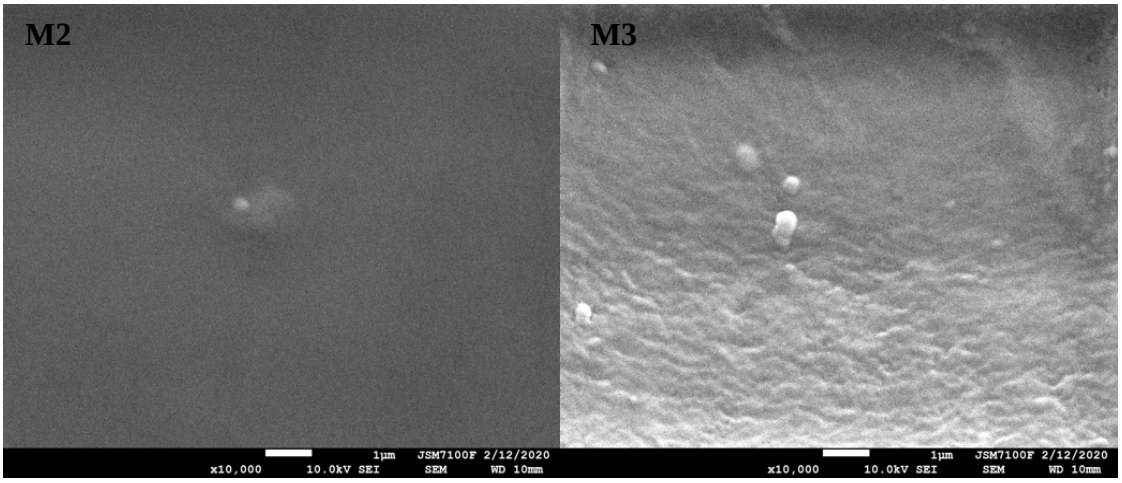

Figure 4. SEM images of the M2 (left) and M3 (right) membranes surfaces (scale bar: 1 μm).

The membrane XRD patterns in the 2θ range 10-80° are reported in Figure 5. As expected, the M1, M2 and M3 membranes were found fully amorphous (the peaks observed were associated

with the adhesive tape used to properly fix the membrane on the sample holder). Still, the results of the M4 membrane were found to be different from those of the other membranes as several peaks belonging to the M4 membrane were detected. These results are in line with ATR-FTIR and SEM analyses as the observed crystallinity can be associated with the TOPO layer formed on the surface of M4 membrane, which was confirmed by comparison with the XRD pattern of the TOPO powder used for membrane preparation (see Figure 6).

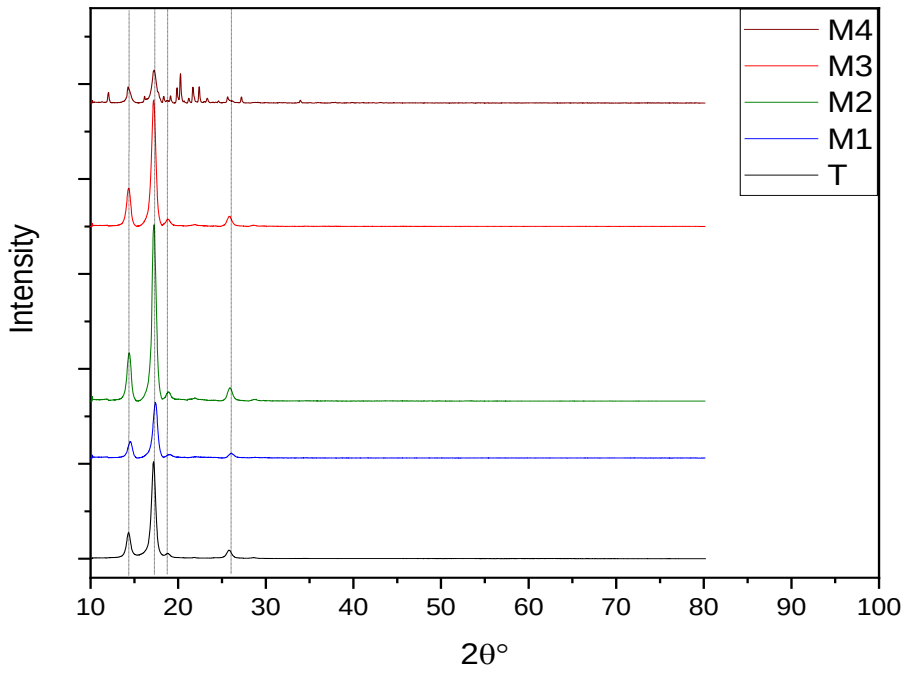

Figure 5. XRD patterns of the various membranes (M1-M4) in the range in the 2θ range 10-80°. The XRD pattern of the adhesive tape (T) used to fix the membranes on the sample holder is also shown for comparison.

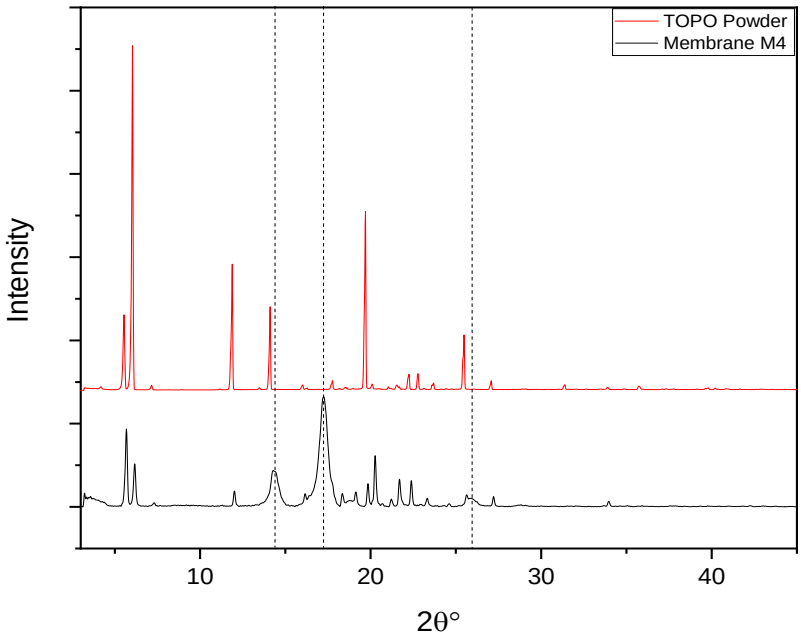

Figure 6. XRD patterns of the M4 membrane and TOPO powder. The dotted vertical lines indicate the peaks associated with the adhesive tape used to fix the membrane.

The results of the membrane electrokinetic characterization are displayed in Figure 7. The reported isoelectric points for CTA membranes are usually below pH 4 [54,55]. The M2, M3 and M4 membranes were found to have isoelectric points around 4.6, 6.1 and 8.6, respectively, while the M1 membrane was positively charged in the whole pH range. The significant decrease in the surface acidity of the various membranes, compared CTA membranes [54,55], results from the addition of PEI in the membrane preparation and the resulting formation of positively charged quaternary ammonium groups [56,29]. It can be noticed that the addition of phosphorus-based additives (D2EHPA and TOPO) led to more basic surfaces (M1 and M4 membranes) compared with membranes containing TDDA and TOA (M2 and M3 membranes, respectively).

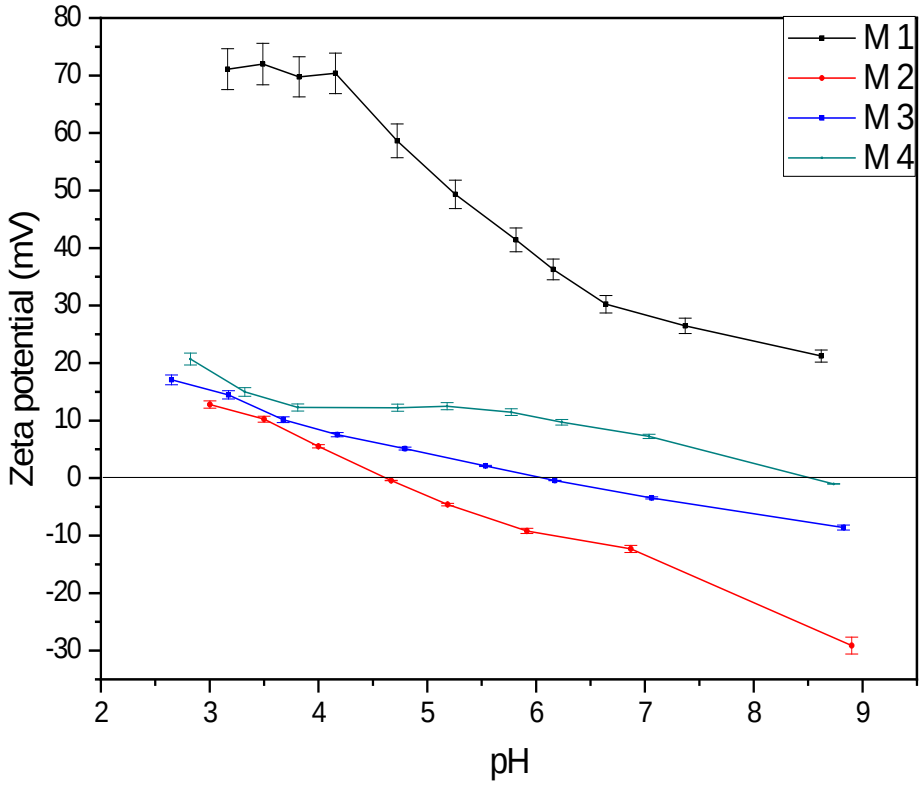

Figure 7. Variation of the zeta potential of the various membranes (M1-M4) with the pH of a 10^{-3} M KCl solution.

3.3 Membrane separation performance

M1-M4 membranes were employed in dialysis experiments to assess their ability to separate boron from REEs (Nd and Pr). The composition of the diluted leachates (see section 2.5) is given in Table 5 (the solutions resulting from leaching of desktop-computer and laptop-computer HDDs are referred to as S1 and S2, respectively).

Table 5. Composition of leachates after dilution. S1 and S2 stand for diluted leachates after desktop-computer-HDD and laptop-computer-HDD lixiviation, respectively. Confidence level: 95 %.

	B (mg/L)	**Fe (mg/L)**	**Pr (mg/L)**	**Nd (mg/L)**
S1	8.724	18.578	35.711	119.141
S2	12.630	129.476	48.142	944.721

As stated in section 2.5, HDD leachates were diluted to attain a pH of ~4 so as to limit the hydrolysis of the acetyl groups of CTA. Furthermore, as shown in Figure 7, this pH guaranteed that all membranes were positively charged, which was expected to be beneficial to prevent transfer of REEs due to strong electrostatic repulsion between the membranes surface and Nd^{3+} and Pr^{3+} ions.

Figures 8a and 8b show the transport yield of the various species (B, Fe, Nd and Pr) contained in solutions S1 and S2, respectively. As a batch cell was used in this study, no steady state could have been reached and values reported in Figures 8 correspond to the membrane performance after a 6-hour dialysis experiment. Although transport yields were found to be dependent on the composition of the feed solution, similar qualitative conclusions could be drawn with the two solutions S1 and S2. Notably, all membranes showed preferential transport of boron over REEs and residual iron. The membranes incorporating phosphorus-based compounds, M1 (CTA / PEI / D2EHPA) and M4 (CTA / PEI / TOPO), were the ones that rejected boron the most strongly. Interestingly, they were also the less hydrated membranes with a water uptake in the range ~6-9 wt. % (see Table 4). As all membranes had a relatively dense structure, it is unlikely that solutes could penetrate the membrane phase while keeping their entire hydration shell [57]. The associated energetic penalty associated with solute partial dehydration could be partly overcome if the solute could interact favorably with water molecules inside the membrane phase. That is why M2 (CTA / PEI / TDDA) and M3 (CTA / PEI / TOA) membranes, which were the most hydrated membranes with a water uptake of 20.3 and 23.1 wt%, respectively (see Table 4), were found to exhibit the highest transport yields for boron. The latter reached almost 15% with the M3 membrane after 6-hour dialysis. It is worth reminding that a batch-cell configuration was used in this work, thus the reported performance could be easily outperformed by optimizing the dialysis cell. These results highlight the great interest of diffusion dialysis for REEs recovery as it is (i) a clean process and (ii) it operates without the energy-intensive application of hydraulic pressure difference or electric field through the membrane but only by spontaneous diffusion, thus making it very attractive in terms of energy savings.

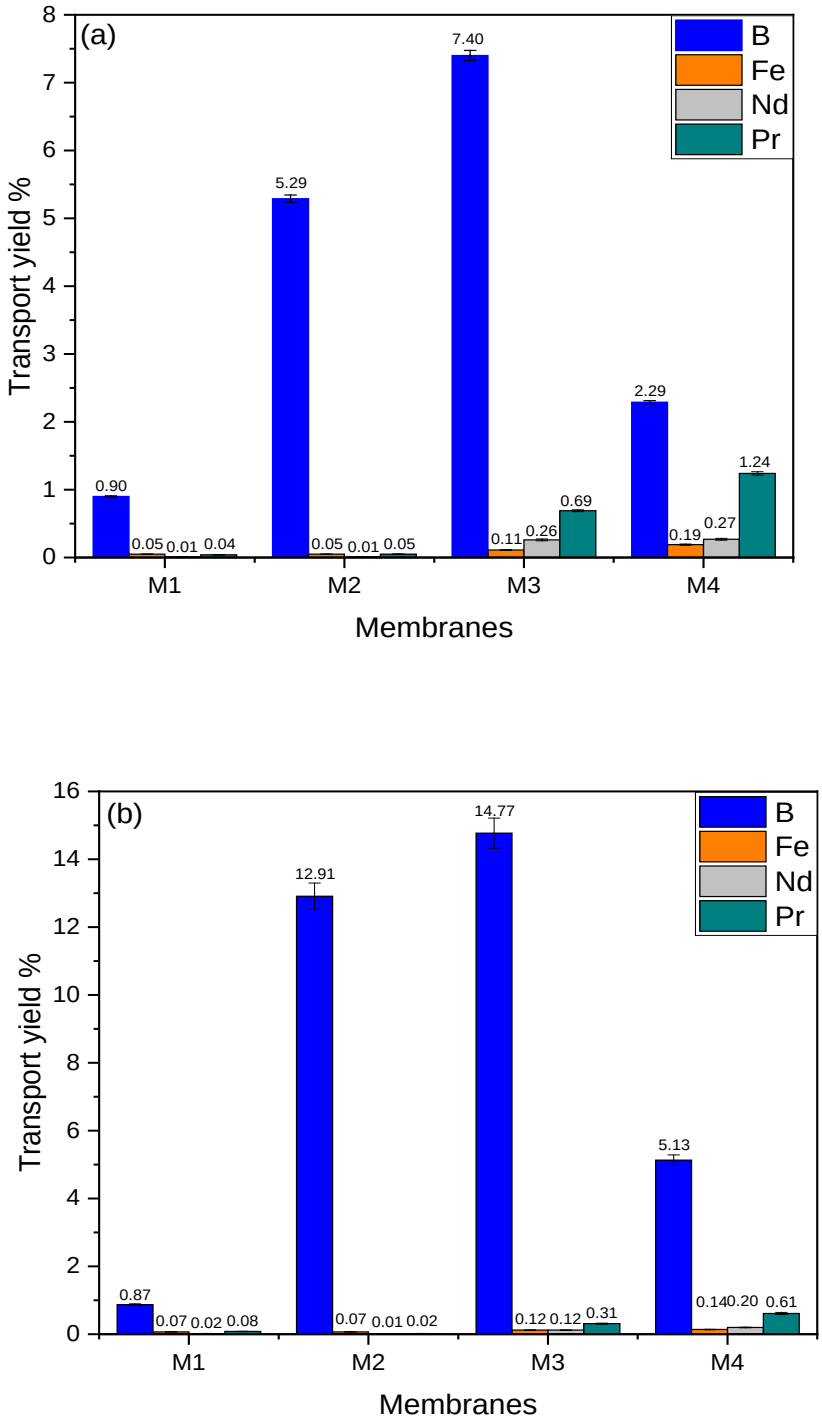

Figure 8. Transport yield of B, Fe, Nd and Pr through the membranes for (a) S1 feed solution and (b) S2 feed solution.

Unlike boron, which was present in the form of uncharged boric acid molecules ($B(OH)_3$ (pK_a = 9.24 at 25 °C), REEs were mainly in the form of trivalent cations (Nd^{3+} and Pr^{3+}) under the conditions of our study [58,59]. The latter were then strongly rejected by the four positively charged membranes. Iron was also strongly rejected by all membranes. As indicated in section 2.5, the increase of pH up to 4 as a result of leachate dilution led to the precipitation of Fe^{3+} ions. It was therefore assumed that the residual iron detected in the leachates after dilution and filtration was in the form of Fe^{2+} ions. As expected, the most strongly charged membrane, M1, exhibited very high REEs rejection. Although the M2 membrane was only slightly positively charged at pH 4 (see Figure 7), it was able to reject REEs at a higher level than the more positively charged M3 and M4 membranes. These results suggest that the M2 membrane had a bit denser structure than M3 and M4. In general, Pr^{3+} cations were transferred slightly more easily across membranes than Nd^{3+}, which may be due to the slightly higher Gibbs energy of hydration of Nd^{3+} (-3280 and -3245 kJ / mol for Nd^{3+} and Pr^{3+}, respectively).

It is noteworthy that D2EHPA and TOPO are known to be efficient to extract REEs when they are used in the liquid / liquid extraction process, in which they are “free” to form coordination complexes with REEs [34,60,61]. However, when embedded into the CTA / PEI polymer matrix, they were found unable to bind with REEs as confirmed by mass balance performed in the feed and stripping compartments of the dialysis cell. It is most probably due to the favorable interaction between the positively charged PEI and the phosphoryl and phosphonyl groups of TOPO and D2EHPA, respectively. Furthermore, the positive membrane charge repelled the like-charged REEs from the membrane surface, thus preventing transport of REEs through the membrane.

M1 and M2 membranes exhibited the highest rejection of REEs but the M1 also strongly rejected boron. As a result, better selectivity factors between B and REEs were reached with the M2 membrane, as reported in Figures 9. Notably, the M2 membrane exhibited an impressive selectivity factor B / Nd in the range 559 – 3706, depending on the leachate composition, which makes it very promising for the recovery of REEs from end-of-life computer hard drives.

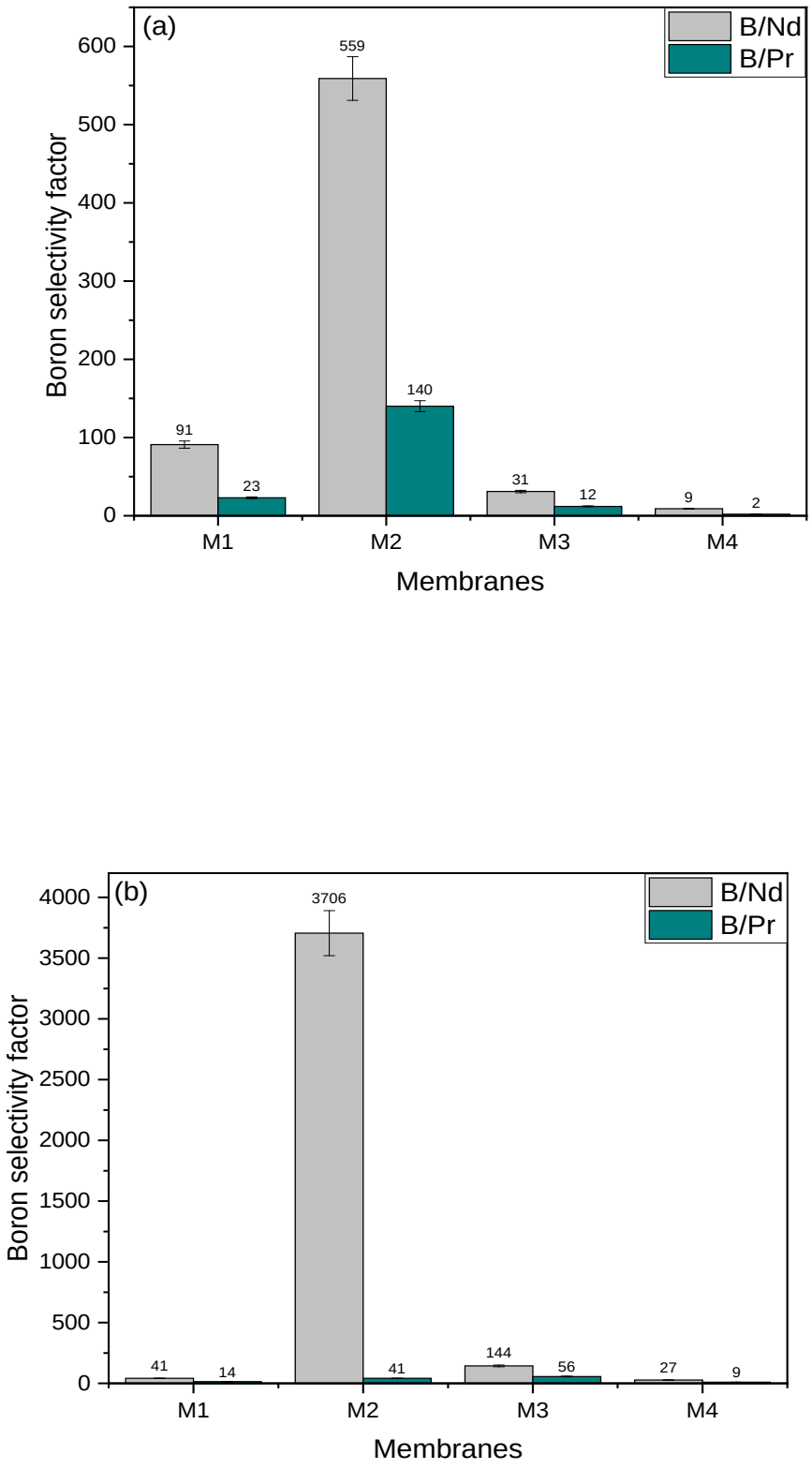

Figure 9. Selectivity factor B / Nd and B / Pr of the various membranes for (a) S1 feed solution and (b) S2 feed solution.

4. Conclusion

Various polymer membranes were synthesized from cellulose triacetate (CTA) and polyethylenimine (PEI) by the solvent evaporation method. Amino-based additives, tridodecylamine (TDDA) and trioctylamine (TOA), and phosphorus-based additives, di-(2-ethylhexyl) phosphoric acid (D2EHPA) and trioctylphosphine oxide (TOPO), were added to the CTA / PEI blends in order to obtain dense membranes with appropriate mechanical properties. Water uptake, contact angle, ATR-FTIR, SEM, XRD and zeta potential techniques were used to characterize the membranes. Unlike TDDA, TOA and D2EHPA, TOPO was found to preferentially migrate towards the membrane surface during the membrane formation process, thus forming a crystalline layer on the membrane surface, as revealed by ATR-FTIR, SEM and XRD analyses.

Nd-Fe-B magnets contained in end-of-life hard disk drives were demagnetized, crushed and grinded before being leached by strong acids. The leachates were further diluted until a pH of ~4 was reached. Setting the pH at this value (i) enabled to limit the hydrolysis of the acetyl groups of CTA, (ii) ensured a positive surface charge for all membranes and (iii) made it possible to remove most of the iron by precipitation of iron(III) hydroxide.

The diluted leachates were then used as feed solutions in diffusion-dialysis experiments and the ability of the various membranes to separate boron from REEs was evaluated. Owing to the positive membrane charge, the transfer of REEs (present in the form of Nd^{3+} and Pr^{3+} cations) was found very small through all membranes. Boron, which was present in the form of neutral boric acid molecules under the operating conditions, was transferred to a greater extent, especially through membranes with high water uptake (i.e. membranes containing an amino-based additive, TDDA or TOA). The CTA / PEI / TOA membrane was able to extract ~15% of the boron after 6-hour dialysis. It should be stressed that this performance could be readily improved as the dialysis experiments were carried out in batch-mode with a lab-scale cell. The CTA / PEI / TDDA membrane had the highest selectivity between boron and neodymium with a B / Nd selectivity factor up to 3706. For all membranes, the selectivity between boron and praseodymium was less than for neodymium (max. 140) because the membranes rejected less strongly Pr^{3+} than Nd^{3+}, which can be understood through their different Gibbs energy of hydration.

This work demonstrated that a clean and energy-efficient process like diffusion dialysis is an attractive alternative method to e.g. liquid / liquid extraction for the recovery of REEs from electronic waste.

Acknowledgements

Francis Gouttefangeas is acknowledged for SEM analyses (UMS 2001 ScanMAT).

References

[1] M. Humphries, “Rare earth elements: The global supply chain,” *Rare Earth Miner. Policies Issues*, pp. 1–20, 2011.

[2] C. Hurst, “China’s Rare Earth Elements Industry: What Can the West Learn? Institute for the Analysis of Global Security (IAGS),” USA, 2010.

[3] L. Omodara, S. Pitkäaho, E. M. Turpeinen, P. Saavalainen, K. Oravisjärvi, and R. L. Keiski, “Recycling and substitution of light rare earth elements, cerium, lanthanum, neodymium, and praseodymium from end-of-life applications - A review,” *Journal of Cleaner Production*, vol. 236. Elsevier Ltd, p. 117573, 01-Nov-2019.

[4] R. Auerbach, K. Bokelmann, R. Stauber, O. Gutfleisch, S. Schnell, and S. Ratering, “Critical raw materials – Advanced recycling technologies and processes: Recycling of rare earth metals out of end of life magnets by bioleaching with various bacteria as an example of an intelligent recycling strategy,” *Miner. Eng.*, vol. 134, pp. 104–117, Apr. 2019.

[5] X. Yin *et al.*, “An Efficient Process for Recycling Nd–Fe–B Sludge as High-Performance Sintered Magnets,” *Engineering*, Nov. 2019.

[6] H. S. Yoon, C. J. Kim, K. W. Chung, S. D. Kim, J. Y. Lee, and J. R. Kumar, “Solvent extraction, separation and recovery of dysprosium (Dy) and neodymium (Nd) from aqueous solutions: Waste recycling strategies for permanent magnet processing,” *Hydrometallurgy*, vol. 165, pp. 27–43, Oct. 2016.

[7] V. Balaram, “Rare earth elements: A review of applications, occurrence, exploration, analysis, recycling, and environmental impact,” *Geosci. Front.*, vol. 10, no. 4, pp. 1285–1303, Jul. 2019.

[8] K. Skotnicova *et al.*, “Structural and magnetic engineering of (Nd, Pr, Dy, Tb)–Fe–B sintered magnets with Tb3Co0.6Cu0.4H composition in the powder mixture,” *J. Magn. Magn. Mater.*, vol. 498, p. 166220, Mar. 2020.

[9] T. T. Sasaki, T. Ohkubo, and K. Hono, “Structure and chemical compositions of the grain boundary phase in Nd-Fe-B sintered magnets,” *Acta Mater.*, vol. 115, pp. 269–277, Aug. 2016.

[10] R. Houot and J.-P. . M. Y. . & S. J.-C. Cuif, “Recovery of Rare Earth Minerals, with Emphasis on Flotation Process | Scientific.Net,” *Mater. Sci. Forum*, vol. 301, no. 24, pp. 70–72, 1991.

[11] A. Jordens, R. S. Sheridan, N. A. Rowson, and K. E. Waters, “Processing a rare earth mineral deposit using gravity and magnetic separation,” *Miner. Eng.*, vol. 62, pp. 9–18, Jul. 2014.

[12] J. Tang and K. H. Johannesson, “Ligand extraction of rare earth elements from aquifer sediments: Implications for rare earth element complexation with organic matter in natural waters,” *Geochim. Cosmochim. Acta*, vol. 74, no. 23, pp. 6690–6705, Dec. 2010.

[13] R. Safarbali, M. R. Yaftian, and A. Zamani, “Solvent extraction-separation of La(III), Eu(III) and Er(III) ions from aqueous chloride medium using carbamoyl-carboxylic acid extractants,” *J. Rare Earths*, vol. 34, no. 1, pp. 91–98, Jan. 2016.

[14] Y. Xia, L. Xiao, J. Tian, Z. Li, and L. Zeng, “Recovery of rare earths from acid leach solutions of spent nickel-metal hydride batteries using solvent extraction,” *J. Rare Earths*, vol. 33, no. 12, pp. 1348–1354, Dec. 2015.

[15] P. K. Parhi, K. H. Park, C. W. Nam, and J. T. Park, “Liquid-liquid extraction and separation of total rare earth (RE) metals from polymetallic manganese nodule leaching solution,” *J. Rare Earths*, vol. 33, no. 2, pp. 207–213, Feb. 2015.

[16] Q. Chen, X. Ma, X. Zhang, Y. Liu, and M. Yu, “Extraction of rare earth ions from phosphate leach solution using emulsion liquid membrane in concentrated nitric acid medium,” *J. Rare Earths*, vol. 36, no. 11, pp. 1190–1197, Nov. 2018.

[17] J. Liu, K. Huang, X. H. Wu, and H. Liu, “Enrichment of Low Concentration Rare Earths from Leach Solutions of Ion-Adsorption Ores by Bubbling Organic Liquid Membrane Extraction Using N1923,” *ACS Sustain. Chem. Eng.*, vol. 5, no. 9, pp. 8070–8078, Sep. 2017.

[18] J. Liu, K. Huang, X. Wu, W. Liu, W. Song, and H. Liu, “Extraction of rare earths using bubbling organic liquid membrane with un-saponified P507,” *Hydrometallurgy*, vol. 175, pp. 340–347, Jan. 2018.

[19] J. López, M. Reig, O. Gibert, and J. L. Cortina, “Integration of nanofiltration membranes in recovery options of rare earth elements from acidic mine waters,” *J. Clean. Prod.*, vol. 210, pp. 1249–1260, Feb. 2019.

[20] J. López, M. Reig, O. Gibert, E. Torres, C. Ayora, and J. L. Cortina, “Application of nanofiltration for acidic waters containing rare earth elements: Influence of transition

elements, acidity and membrane stability," *Desalination*, vol. 430, pp. 33–44, Mar. 2018.

[21] Z. Chen, J. Xu, F. Sang, and Y. Wang, "Efficient extraction and stripping of Nd(III), Eu(III) and Er(III) by membrane dispersion micro-extractors," *J. Rare Earths*, vol. 36, no. 8, pp. 851–856, Aug. 2018.

[22] Z. Chen, F. N. Sang, J. H. Xu, G. S. Luo, and Y. D. Wang, "Efficient enrichment and recovery of rare earth elements with low concentration by membrane dispersion micro-extractors," *Chem. Eng. Process. - Process Intensif.*, vol. 127, pp. 127–135, May 2018.

[23] T. Hango, M. Goto, and F. Nakashio, "Extraction Kinetics of Rare Earth Metals with 2-Ethylhexyl Phosphonic Acid Mono-2-ethylhexyl Ester Using a Hollow Fiber Membrane Extractor," *Sep. Sci. Technol.*, vol. 30, no. 5, pp. 777–792, 1995.

[24] J. Luo, C. Wu, T. Xu, and Y. Wu, "Diffusion dialysis-concept, principle and applications," *J. Memb. Sci.*, vol. 366, no. 1–2. Elsevier, pp. 1–16, 01-Jan-2011.

[25] S. Lahiri and S. Sarkar, "Separation of iron and cobalt using 59Fe and 60Co by dialysis of polyvinylpyrrolidone-metal complexes: A greener approach," *Appl. Radiat. Isot.*, vol. 65, no. 4, pp. 387–391, Apr. 2007.

[26] S. Bensaadi *et al.*, "Dialysis and photo-electrodialysis processes using new synthesized polymeric membranes for the selective removal of bivalent cations," *J. Environ. Chem. Eng.*, vol. 5, no. 1, pp. 1037–1047, Feb. 2017.

[27] O. Kebiche-Senhadji, L. Mansouri, S. Tingry, P. Seta, and M. Benamor, "Facilitated Cd(II) transport across CTA polymer inclusion membrane using anion (Aliquat 336) and cation (D2EHPA) metal carriers," *J. Memb. Sci.*, vol. 310, no. 1–2, pp. 438–445, Mar. 2008.

[28] S. Bensaadi, O. Arous, H. Kerdjoudj, and M. Amara, "Evaluating molecular weight of PVP on characteristics of CTA membrane dialysis," *J. Environ. Chem. Eng.*, vol. 4, no. 2, pp. 1545–1554, Jun. 2016.

[29] M. Bagheri *et al.*, "Preparation of a positively charged NF membrane by evaporation deposition and the reaction of PEI on the surface of the C-PES/PES blend UF membrane," *Prog. Org. Coatings*, vol. 141, p. 105570, Apr. 2020.

[30] M. Amara and H. Kerdjoudj, "Modification of cation-exchange membrane properties by electro-adsorption of polyethyleneimine," *Desalination*, vol. 155, no. 1, pp. 79–87, May 2003.

[31] A. Gherrou, H. Kerdjoudj, R. Molinari, and E. Drioli, "Removal of silver and copper ions from acidic thiourea solutions with a supported liquid membrane containing

D2EHPA as carrier," *Sep. Purif. Technol.*, vol. 28, no. 3, pp. 235–244, Sep. 2002.

[32] N. Bayou, O. Arous, M. Amara, and H. Kerdjoudj, "Elaboration and characterisation of a plasticized cellulose triacetate membrane containing trioctylphosphine oxyde (TOPO): Application to the transport of uranium and molybdenum ions," *Comptes Rendus Chim.*, vol. 13, no. 11, pp. 1370–1376, Nov. 2010.

[33] O. Arous, M. Amara, M. Trari, A. Bouguelia, and H. Kerdjoudj, "Cadmium (II) and lead (II) transport in a polymer inclusion membrane using tributyl phosphate as mobile carrier and CuFeO2 as a polarized photo electrode," *J. Hazard. Mater.*, vol. 180, no. 1–3, pp. 493–498, Aug. 2010.

[34] S. Wu *et al.*, "Simultaneous recovery of rare earths and uranium from wet process phosphoric acid using solvent extraction with D2EHPA," *Hydrometallurgy*, vol. 175, pp. 109–116, Jan. 2018.

[35] M. K. Jha, A. Kumari, R. Panda, J. Rajesh Kumar, K. Yoo, and J. Y. Lee, "Review on hydrometallurgical recovery of rare earth metals," *Hydrometallurgy*, vol. 165, pp. 2–26, Oct. 2016.

[36] L. D. Nghiem, P. Mornane, I. D. Potter, J. M. Perera, R. W. Cattrall, and S. D. Kolev, "Extraction and transport of metal ions and small organic compounds using polymer inclusion membranes (PIMs)," *J. Memb. Sci.*, vol. 281, no. 1–2. Elsevier, pp. 7–41, 15-Sep-2006.

[37] C. V. I. Gherasim, G. Bourceanu, R. I. Olariu, and C. Arsene, "Removal of lead(II) from aqueous solutions by a polyvinyl-chloride inclusion membrane without added plasticizer," *J. Memb. Sci.*, vol. 377, no. 1–2, pp. 167–174, Jul. 2011.

[38] G. D. Rodrigues, M. do C. H. da Silva, L. H. M. da Silva, F. J. Paggioli, L. A. Minim, and J. S. dos Reis Coimbra, "Liquid-liquid extraction of metal ions without use of organic solvent," *Sep. Purif. Technol.*, vol. 62, no. 3, pp. 687–693, Sep. 2008.

[39] Y. Zhang *et al.*, "Squareness factors of demagnetization curves for multi-main-phase Nd-Ce-Fe-B magnets with different Ce contents," *J. Magn. Magn. Mater.*, vol. 487, p. 165355, Oct. 2019.

[40] M. Sugiura, M. Kikkawa, and S. Urita, "Carrier-mediated transport of rare earth ions through cellulose triacetate membranes," *J. Memb. Sci.*, vol. 42, no. 1–2, pp. 47–55, Mar. 1989.

[41] M. Sugiura, "Transport of lanthanide ions through cellulose triacetate membranes containing hinokitiol and flavonol as carriers," *Sep. Sci. Technol.*, vol. 25, no. 11–12, pp. 1189–1199, 1990.

[42] I. Soroko, M. Makowski, F. Spill, and A. Livingston, “The effect of membrane formation parameters on performance of polyimide membranes for organic solvent nanofiltration (OSN). Part B: Analysis of evaporation step and the role of a co-solvent,” *J. Memb. Sci.*, vol. 381, no. 1–2, pp. 163–171, Sep. 2011.

[43] I. Prihatiningtyas, Y. Li, Y. Hartanto, A. Vananroye, N. Coenen, and B. Van der Bruggen, “Effect of solvent on the morphology and performance of cellulose triacetate membrane/cellulose nanocrystal nanocomposite pervaporation desalination membranes,” *Chem. Eng. J.*, vol. 388, p. 124216, May 2020.

[44] Y. Hanafi *et al.*, “Electrokinetic analysis of PES/PVP membranes aged by sodium hypochlorite solutions at different pH,” *J. Memb. Sci.*, vol. 501, pp. 24–32, Mar. 2016.

[45] P. Fievet, M. Sbaï, A. Szymczyk, C. Magnenet, C. Labbez, and A. Vidonne, “A new tangential streaming potential setup for the electrokinetic characterization of tubular membranes,” *Sep. Sci. Technol.*, vol. 39, no. 13, pp. 2931–2949, 2004.

[46] A. M. Farooque, A. Al-Amoudi, and K. Numata, “Degradation study of cellulose triacetate hollow fine-fiber SWRO membranes,” *Desalination*, vol. 123, no. 2–3, pp. 165–171, Oct. 1999.

[47] G. M. Geise, H. S. Lee, D. J. Miller, B. D. Freeman, J. E. McGrath, and D. R. Paul, “Water purification by membranes: The role of polymer science,” *J. Polym. Sci. Part B Polym. Phys.*, vol. 48, no. 15, pp. 1685–1718, Aug. 2010.

[48] H. Yan, S. Xue, C. Wu, Y. Wu, and T. Xu, “Separation of NaOH and NaAl(OH)4 in alumina alkaline solution through diffusion dialysis and electrodialysis,” *J. Memb. Sci.*, vol. 469, pp. 436–446, Nov. 2014.

[49] A. Ikram *et al.*, “The sintering mechanism of fully dense and highly coercive Nd-Fe-B magnets from the recycled HDDR powders reprocessed by spark plasma sintering,” *J. Alloys Compd.*, vol. 774, pp. 1195–1206, Feb. 2019.

[50] C. R. Dias, M. J. Rosa, and M. N. De Pinho, “Structure of water in asymmetric cellulose ester membranes - An ATR-FTIR study,” *J. Memb. Sci.*, vol. 138, no. 2, pp. 259–267, Jan. 1998.

[51] M. R. Kotte, M. Cho, and M. S. Diallo, “A facile route to the preparation of mixed matrix polyvinylidene fluoride membranes with in-situ generated polyethyleneimine particles,” *J. Memb. Sci.*, vol. 450, pp. 93–102, Jan. 2014.

[52] F. Zarei *et al.*, “Preparation of thin film composite nano-filtration membranes for brackish water softening based on the reaction between functionalized UF membranes and polyethyleneimine,” *J. Memb. Sci.*, vol. 588, p. 117207, Oct. 2019.

[53] V. V. T. Doan-Nguyen, P. J. Carroll, and C. B. Murray, “Structure determination and modeling of monoclinic trioctylphosphine oxide,” *Acta Crystallogr. Sect. C Struct. Chem.*, vol. 71, no. 3, pp. 239–241, Mar. 2015.

[54] T. P. N. Nguyen, E. T. Yun, I. C. Kim, and Y. N. Kwon, “Preparation of cellulose triacetate/cellulose acetate (CTA/CA)-based membranes for forward osmosis,” *J. Memb. Sci.*, vol. 433, pp. 49–59, Apr. 2013.

[55] T. P. N. Nguyen, B. M. Jun, and Y. N. Kwon, “The chlorination mechanism of integrally asymmetric cellulose triacetate (CTA)-based and thin film composite polyamide-based forward osmosis membrane,” *J. Memb. Sci.*, vol. 523, pp. 111–121, Feb. 2017.

[56] P. Xu *et al.*, “Positive charged PEI-TMC composite nanofiltration membrane for separation of Li+ and Mg2+ from brine with high Mg2+/Li+ ratio,” *Desalination*, vol. 449, pp. 57–68, Jan. 2019.

[57] M. Ding, A. Szymczyk, and A. Ghoufi, “On the structure and rejection of ions by a polyamide membrane in pressure-driven molecular dynamics simulations,” *Desalination*, vol. 368, pp. 76–80, Jul. 2015.

[58] A. A. Migdisov and A. E. Williams-Jones, “A spectrophotometric study of neodymium(III) complexation in chloride solutions,” *Geochim. Cosmochim. Acta*, vol. 66, no. 24, pp. 4311–4323, Dec. 2002.

[59] L. Liu, G. Tian, and L. Rao, “Effect of Solvation? Complexation of Neodymium(III) with Nitrate in an Ionic Liquid (BumimTf2N) in Comparison with Water,” *Solvent Extr. Ion Exch.*, vol. 31, no. 4, pp. 384–400, Jul. 2013.

[60] S. Radhika, B. N. Kumar, M. L. Kantam, and B. R. Reddy, “Liquid-liquid extraction and separation possibilities of heavy and light rare-earths from phosphoric acid solutions with acidic organophosphorus reagents,” *Sep. Purif. Technol.*, vol. 75, no. 3, pp. 295–302, Nov. 2010.

[61] A. Battsengel, A. Batnasan, A. Narankhuu, K. Haga, Y. Watanabe, and A. Shibayama, “Recovery of light and heavy rare earth elements from apatite ore using sulphuric acid leaching, solvent extraction and precipitation,” *Hydrometallurgy*, vol. 179, pp. 100–109, Aug. 2018.